Article

Why Are Mixed Alkali Metal Cation Salts Formed? The [W(CN)$_6$(bpy)]$^{2-}$ Case: Structural Study

Maciej Hodorowicz,* Janusz Szklarzewicz, and Anna Jurowska

Read Online

ACCESS | Metrics & More | Article Recommendations | Supporting Information

ABSTRACT: In this article, we show how compounds based on a little-known (unexplored) anionic 6-cyanido building block, [W-(CN)$_6$(bpy)]$^{2-}$, can vary their network architecture as a result of interactions between the bridging cyanido ligands and alkali metal cations in so-called "coordination polymers". This paper describes the synthesis and structural studies of anionic 6-cyanido tungstates with various alkali heterocation systems Me$^+$/Me$^{+\prime}$ [(where Me$^+$/Me$^{+\prime}$ = Na$^+$, K$^+$, (**1**); Na$^+$, Rb$^+$, (**2**); Na$^+$, Cs$^+$ (**3**)], and it is shown that typical "end-on" interactions between cyanido ligands and Na$^+$ cations are enhanced by more unusual "side-on" interactions resulting from the presence of soft metal cations (K$^+$, Rb$^+$, and Cs$^+$). This results in the formation of much more complex structures with an increased number of intermolecular interactions and, consequently, also lower solubility of mixed cation salts compared to all homocationic salts. A comparative structural analysis with all homocationic analogues of Na, K, Rb, and Cs published to date is presented and discussed.
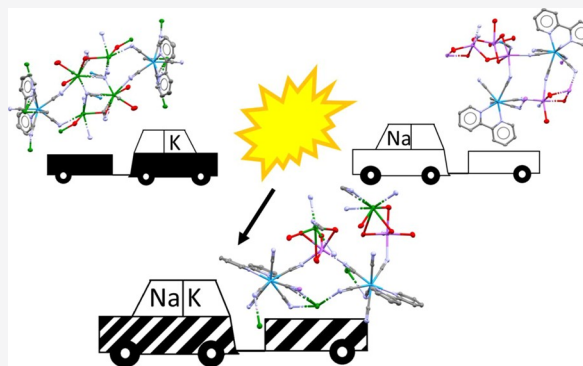
INTRODUCTION

Mixed salts of alkali metal cations are known from the very beginning of chemistry. One of the best known is the sodium/potassium tartrate, NaKC$_4$H$_4$O$_6$·4H$_2$O, known as Seignette's or Rochelle's salt.[1] In the case of cyanido complexes, the salts of the formula NaK$_3$[M(CN)$_4$O$_2$]·6H$_2$O (where M = Mo or W) are well known.[2,3] The main question is how is the correct cation ratio obtained? For Seignette's salt, it is a stoichiometric reaction of HKC$_4$H$_4$O$_6$ with NaHCO$_3$; however, in the case of the mentioned Mo and W tetracyanido complexes, it is the preferred form of crystals because of their lower solubility. Therefore, there must be a structural reason for stronger cation−anion interactions of mixed cationic salts as compared to monocation analogues, at least for some anions. There are hardly any publications related to this intriguing subject, possibly due to problems with good-quality crystal formation for these two types of salts of the same anion. For example, in the case of the NaK$_3$[M(CN)$_4$O$_2$]·6H$_2$O salt, pure sodium salts form oils or crystals of a quality unsuitable for structural measurements, while pure potassium salts do not crystallize at all. In our recent articles, we have described the salts of the anion [W(CN)$_6$(bpy)]$^{2-}$ with all alkali metals except radio-active francium.[4−7] We found that the sodium salt is the least soluble among them, and interestingly, the addition of K$^+$, Rb$^+$, or Cs$^+$ cations to it does not separate the corresponding potassium to cesium salts but causes the formation of mixed cationic crystals, Na:K/Rb/Cs with a composition that the molar ratio is 1:1, except 1:3 for Cs. Because the crystals of the obtained salts were suitable for X-ray diffraction measure-

ments, we decided to compare the structures of the obtained compounds and try to answer the question why such precisely stoichiometric mixed cation salts are so easy to isolate.

The anionic complex [W(CN)$_6$(bpy)]$^{2-/−}$ as a structural element in crystal engineering is rarely used in the design and synthesis of bimetallic systems, which is mainly due to the difficult and time-consuming synthesis that requires a lot of intuition and experience. However, the said tungsten 6-cyanido (IV/V) system has several advantages generally under-estimated by numerous researchers. In contrast to its 8-cyanido counterpart, it has a planar bipyridyl bidentate ligand molecule that replaced the two cyanido ligands, resulting in a lower negative anion charge and blocking of two potentially bridging sites. The lower anion charge determines the different stoichiometry of the bimetallic assemblies (table). It should be noted that the lower charge makes the 6-cyanido system more soluble in nonaqueous solutions, and blocking the two sites with potential bridging properties consequently leads to systems with a lower lattice dimensionality, making them simpler and easier to interpret. In addition, the 6-cyanido anion modified with the bidentate ligand is extremely rigid, and

Table 1. Crystal Data and Structure Refinement for 1−3

	1	2	3
empirical formula	$C_{16}H_{12}KN_8NaO_5W$	$C_{16}H_{18}N_8NaO_5RbW$	$C_{32}H_{16}Cs_3N_{16}NaO_8W_2$
formula weight	642.28	694.69	1542.03
temperature [K]	130(2)	130.00(10)	130(2)
wavelength [Å]	0.71073	0.71073	0.71073
crystal system	monoclinic	monoclinic	triclinic
space group	$P2_1/n$	$P2_1/n$	$P\bar{1}$
a [Å]	8.2425 (2)	8.41800(10)	9.30800(10)
b [Å]	27.1941 (7)	27.4644(4)	15.9060(2)
c [Å]	10.3067(3)	10.0963(2)	17.0563(2)
α [deg]	90	90	114.4630(10)
β [deg]	103.386(3)	102.470(2)	93.9120(10)
γ [deg]	90	90	97.3070(10)
volume [Å^3]	2247.46(11)	2279.15(6)	2259.34(5)
Z	4	4	2
density (calculated) [Mg/m^3]	1.898	2.025	2.267
absorption coefficient [mm^{-1}]	5.389	7.254	7.543
$F(000)$	1232	1328	1416
crystal size [mm^3]	$0.20 \times 0.15 \times 0.05$	$0.20 \times 0.15 \times 0.10$	$0.15 \times 0.10 \times 0.10$
θ range for data collection [deg]	2.165 to 31.822	2.543 to 28.647	2.226 to 31.900
index ranges	$-11 \leq h \leq 10$	$-11 \leq h \leq 11$	$-12 \leq h \leq 13$
	$-40 \leq k \leq 37$	$-36 \leq k \leq 36$	$-23 \leq k \leq 23$
	$-14 \leq l \leq 14$	$-13 \leq l \leq 11$	$-24 \leq l \leq 24$
reflections collected	68,508	20,384	76,246
independent reflections	7023 [$R_{int} = 0.0758$]	5394 [$R_{int} = 0.0390$]	13,493 [$R_{int} = 0.0812$]
completeness to θ [%]	99.9	99.8	99.9
refinement method	full-matrix least-squares on F^2	full-matrix least-squares on F^2	full-matrix least-squares on F^2
data/restraints/parameters	7023/0/291	5394/2/329	13,493/0/559
goodness of fit on F^2	1.040	1.077	1.057
final R indices [$I > 2\sigma(I)$]	$R_1 = 0.0299$	$R_1 = 0.0251$	$R_1 = 0.0401$
	$wR_2 = 0.0700$	$wR_2 = 0.0531$	$wR_2 = 0.1097$
R indices (all data)	$R_1 = 0.0388$	$R_1 = 0.0298$	$R_1 = 0.0483$
	$wR_2 = 0.0733$	$wR_2 = 0.0549$	$wR_2 = 0.1143$
largest diff. peak and hole [e·Å^{-3}]	2.764 and −1.627	0.958 and −1.617	3.760 and −2.764

its geometry is not influenced by the environment, making it a predictable building unit in crystal engineering.[4−8] The closest 8-coordinating cyanido relatives, the $[M(CN)_8]^{n-}$ anions, (M = Mo, W, Nb) show relatively high geometric flexibility, which is connected with the low energy barrier between different coordination polyhedra. The presence of eight potentially bridging cyanido ligands and large charge [3− for Mo(V) and W(V)] makes them useful building blocks in the synthesis of coordination polymers.[9−12] Therefore, similar to previous studies, we also focus on the detailed structural characteristics of the first synthesized trimetallic compounds containing mixed alkali metal cations on the precursor [W-(CN)$_6$(bpy)]$^{2-/-}$. We present the description of the synthesis and explain the scheme of creating a layered structure of the obtained systems in correlation with the bridging properties occurring in the structures of building units. Such a detailed structural analysis is important for one more reason, that is, in the described structures there are various, rarely observed simultaneously in one structure, modes of cyanido ligand coordination with its N-end, which affects numerous physical properties exhibited by the complexes, including magnetic properties.[13−18]

■ EXPERIMENTAL SECTION

(PPh$_4$)$_2$[W(CN)$_6$(bpy)]·4H$_2$O and Me$_2$[W(CN)$_6$(bpy)] (Me = Na, K, Rb or Cs) were synthesized as we described earlier.[4,6,7,19,20] NaCl,

KCl, RbCl, CsCl, and all other chemicals were of analytical grade (Aldrich) and were used as supplied. Microanalyses of carbon, hydrogen, and nitrogen were performed using an Elementar Vario MICRO Cube elemental analyzer. IR spectra were recorded on a Nicolet iS5 FT-IR spectrophotometer.

Synthesis of NaK[W(CN)$_6$(bpy)]·5H$_2$O (1). Method (a) the sodium salt, Na$_2$[W(CN)$_6$(bpy)]·xH$_2$O (50 mg), was dissolved in a minimal amount of water (2 mL), and solid KCl (20 mg) was then added. The resulting crystals were filtered off and washed with a minimal amount of water-acetone (1:1 v/v) mixture and next with pure acetone. The crystals for X-ray measurements were taken from solution before filtration.

Method (b) the procedure was identical as that in (a), but potassium salt was used instead of sodium one, and NaCl (20 mg) was used instead of KCl. Anal. calcd for $C_{16}H_{18}KN_8NaO_5W$: C, 29.64; N, 17.28; H, 2.80%. Found: C, 29.68, N, 17.21; H, 2.36% IR-ATR ν_{CN} (cm^{-1}): 2120 (s), 2137 (m), 2161 (w).

Synthesis of NaRb[W(CN)$_6$(bpy)]·5H$_2$O (2). The procedures a and b were analogous to that described for **1**. Rubidium chloride (RbCl, 30 mg) was used instead of potassium chloride. Anal. calcd for $C_{16}H_{18}RbN_8NaO_5W$·2RbCl: C, 20.52; N, 11.97; H, 1.94%. Found: C, 20.28, N, 12.08; H, 1.50%. IR-ATR ν_{CN} (cm^{-1}): 2119 (s), 2137 (m), 2161 (w).

Synthesis of NaCs$_3${[W(CN)$_6$(bpy)]}$_2$·8H$_2$O (3). The procedures a and b were analogous to that described for **1** or **2**. Cesium chloride (CsCl, 30 mg) was used instead of potassium one. Anal. calcd for $C_{32}H_{32}Cs_3N_{16}NaO_8W_2$·0.5CsCl: C, 23.40; N, 13.65; H, 1.96%. Found: C, 23.46, N, 13.65; H, 1.77%. IR-ATR ν_{CN} (cm^{-1}): 2109 (s), 2117 (m), 2132 (m), 2151 (w), 2163 (w).

Crystallographic Data Collection and Structure Refinement. Diffraction intensity data for single crystals of three new compounds were collected: for **1** and **3** at 130 K on a Rigaku XtaLAB Synergy-S diffractometer with mirror-monochromated Mo Kα radiation and for **2** at 130 K on an Oxford Diffraction Super Nova diffractometer using monochromatic Mo Kα radiation, λ = 0.71073 Å. Cell refinement and data reduction were performed using firmware.[21] Positions of all of the nonhydrogen atoms were determined by direct methods using SHELXL-2017/1.[22,23] All nonhydrogen atoms were refined anisotropically using weighted full-matrix least-squares on F^2. Refinement and further calculations were carried out using SHELXL-2017/1.[22,23] All hydrogen atoms joined to carbon atoms were positioned with idealized geometries and refined using a riding model with U_{iso}(H) fixed at 1.2 U_{eq} (C$_{arom}$). The figures were made using Diamond ver. 4.6.1 software.[24] CCDC 2113721, 1908247, and 2113722 contain the supplementary crystallographic data for **1**, **2**, and **3**. These data can be obtained free of charge from The Cambridge Crystallographic Data Centre via www.ccdc.cam.ac.uk/data_request/cif.

RESULTS AND DISCUSSION

General Remarks to the Synthesis. The addition of chloride salts of K$^+$, Rb$^+$, or Cs$^+$ cations to a concentrated solution of Na$_2$[W(CN)$_6$(bpy)] results in the formation of well-shaped crystals of **1−3** with yields of ca. 60%. Salts can be also obtained from their potassium, rubidium, or cesium salts of [W(CN)$_6$(bpy)]$^{2-}$ anions by addition of NaCl. The X-ray crystal structure parameters of crystals obtained in method a or b were found to be identical within experimental error. In general, there are problems with separation of crystals as they are very well soluble in water and insoluble in organic solvents; thus they cannot be washed. This results in problems with elemental analysis as crystals are contaminated with alkali metal chlorides. For crystal structure measurements, the crystals were taken directly from mother liquor, the IR spectra were measured on single crystals or on samples washed with acetone, and the alkali metal chloride contaminants do not have any bands in the IR range used. IR spectra of **1−3** are presented in Figures S1−S3, while the ν_{CN} bands are given in the Experimental Section part.

Description of the Structures. The crystal data and structure refinement parameters for complexes **1−3** are collected in Table 1. The selected bond distances and angles are summarized in Table S1.

Anion Structure. The anionic complex [W(CN)$_6$(bpy)]$^{2-}$ in all described compounds, **1−3**, has a dodecahedron geometry, as shown in Figure 1 on the example of compound **1**.

The C13−N13 cyanido ligand in structure **1** is slightly tilted toward the bpy ligand (71.04°), whereas the other cyanido ligands face outward from the bpy ligand. An analogous geometrical fact is observed in the anionic complexes of the other structures described. This type of slope of the single cyanido ligand toward the plane of the bpy ligand is also observed for previously published compounds containing [W^{IV}(CN)$_6$(bpy)]$^{2-}$[4−8] and [W^V(CN)$_6$(bpy)]$^-$,[25] but the slope is 2−3° greater in the case of W^V. The N1, N12, and C16 atoms form a plane relative to which the W1 tungsten atom is shifted by 0.201 Å toward the C13 atom. Analogous shifts are observed for compounds **2** and **3** and are 0.159 and 0.156 Å, respectively. It is worth noting that for structures with W^V these shifts are more pronounced[25] and are for the unmixed systems: for Na = 2.67 Å, for K = 0.250 Å, and for Rb = 0.247 Å. In both cases, that is, W^{IV} and W^V, a decreasing trend in the deformation of the geometry of the anionic
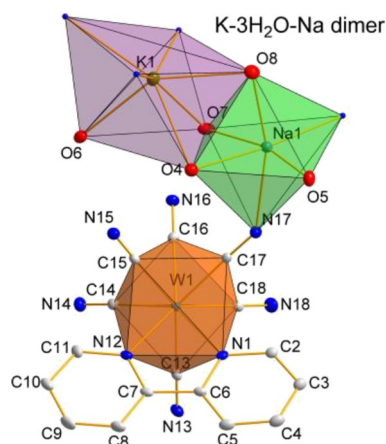
Figure 1. Structure of an anionic complex molecule [W-(CN)$_6$(bpy)]$^{2-}$ on the example of structure **1** with the adopted numbering scheme. The coordination environment around the tungsten atom is in the shape of a slightly distorted dodecahedron. All H atoms are omitted for clarity. All nonhydrogen atoms are represented at 30% probability thermal ellipsoids.

complex is clearly visible with increasing ionic radius of the cation.

The average W−C distances for all six ligands in structures **1**, **2**, and **3** are 2.154, 2.156, and 2.157 Å, respectively, and based on previous studies, it can be concluded that there is no influence of the cation type or structure spatial arrangement on the W−C distance. However, it should be noted that for all the systems of this type studied, the W−C distance for the cyanido ligand being in a perpendicular position with respect to the bpy (for **1** it is C13−N13) is always slightly longer with respect to the other cyanides. The situation is similar for the W−N (cyanido nitrogen) distance, where the average length is 3.30 ± 0.01 Å, regardless of the type of cation and also for N13 (in **1**) and its counterparts in the other structures the mentioned distance is slightly longer. The W−N$_{bpy}$ distances are not significantly different between the salts of W^{IV} and W^V analogues. The bipyridyl ligand (bpy) present in the structures has an almost completely flat molecular geometry.

On the basis of the analysis of the geometry of all published so far systems containing the anionic complex [W$^{IV/V}$(CN)$_6$(bpy)]$^{2-/-}$, it can be concluded that the geometry of the mentioned anion is almost insensitive to the type of counter ion and packing of the structure. Only subtle geometrical trends, slightly more pronounced in the case of the W^V anion, manifested by a slightly larger perturbation of the anion geometry, are visible. Thus, it is not possible to distinguish unambiguously the degree of tungsten oxidation in the studied anions.

Structure of 1 (NaK). Compound **1** crystallizes in the monoclinic space group P2$_1$/n, and the asymmetric part of the unit cell (shown in Figure 1) contains the complex anion [W(CN)$_6$(bpy)]$^{2-}$, two cations, Na$^+$ and K$^+$, and five solvating (coordinating) cations of water molecules. These alkali cations form a dimeric system in which three water molecules form bridges between the cations. The coordination environment around the sodium ion adopts octahedral geometry, with the three corners of the polyhedron being bridged water molecules, while the other three coordination sites are occupied by the fourth water molecule (O5) and two nitrogen atoms from the cyanido ligands, N17 and N18, which is

derived from the cyanido ligand symmetrically dependent anion.

The environment of the potassium cation can be considered as seven-coordinate adopting the geometry of the deformed capped trigonal prism,[26] with three places occupied by bridging waters, while the other four are occupied by one water molecule (O6) and three cyanido ligands (C14N14, C16N16, and C18N18) forming cyanido "side-on" bridges for potassium (Figure 2).
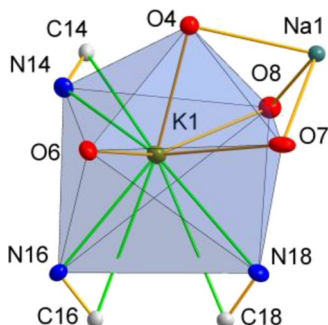
Figure 2. Coordination surroundings of the potassium cation with visible bridging interactions of the "side-on" type (green).

Figure 3 shows the spatial arrangement of tungsten atoms, which as anionic complexes form ribbons running in the [100]
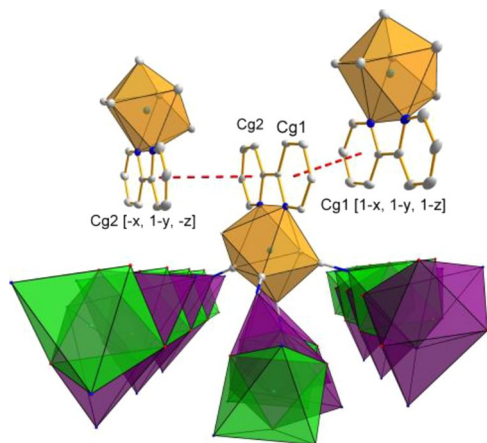

Figure 3. Interactions of a single anion $[W(CN)_6(bpy)]^{2-}$, with three cationic K-3H$_2$O-Na chains and adjacent tungsten ribbons through $\pi-\pi$ interactions (red dashed lines). Color scheme as in Figure 1.

direction. Tungsten ribbons are connected by $\pi-\pi$ interactions of bpy ligands from adjacent ribbons. Each anionic complex $[W(CN)_6(bpy)]^{2-}$ is bound via cyanido bridging interactions by three polymeric cationic chains in which the repeating basic unit is the cationic K-3H$_2$O-Na dimer. The cationic chain is not perfectly straight; it has a zigzag pattern with a K−Na−K angle of 159.94 (4)°.

Each anionic complex through four cyanido ligands is involved in the formation of three "side-on" type bridges to potassium cations only and two "end-on" type bridges to Na$^+$ only (Figure 4), of which the C16N16 ligand forms a bifurcated bridge. Two cyanido ligands, C13N13 and C15N15, are not involved in any bridging interactions.

When analyzing the packing of structure **1**, it can be seen that it adopts a two-layer arrangement, with an "organic" layer
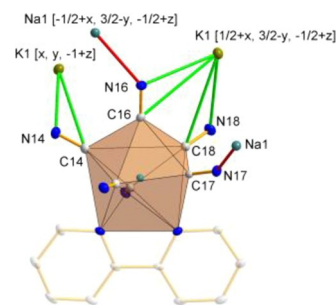
Figure 4. Anion bridge interactions $[W(CN)_6(bpy)]^{2-}$, in structure **1**. Green are "side-on" bridges to potassium cations, and red are "end-on" bridges to sodium cations. The cyanido ligand C15N15 not involved in bridging interactions is in the foreground, while C13N13, hidden by the coordination polyhedron, does not participate in the formation of bridge interactions in any so far known anion-containing structure $[W(CN)_6(bpy)]^{2-}$. The first case is the structure **3**.

made of bpy ligands interacting through $\pi-\pi$ type interactions (Table 2) and of an "inorganic" layer in which the cations K$^+$

Table 2. $\pi\cdots\pi$ Interactions for 1, 2, and 3

$\pi\cdots\pi$	$d(\pi\cdots\pi)$ [Å]	shift [Å]	
1 Na/K			
Cg1⋯Cg1	3.696(1)	1.244	Cg1: N1−C2−C3−C4−C5−C6
Cg2⋯Cg2 [1 − X, −Y, 1 − Z]	3.983(1)	1.891	Cg2: N12−C7−C8−C9−C10−C11
2 Na/Rb			
Cg2⋯Cg2 [1 − X, 1 − Y, 2 − Z]	3.712(2)	1.394	Cg2: N12−C7−C8−C9−C10−C11
3 Na/Cs			
Cg1⋯Cg2 [1 − X, −Y, 1 − Z]	4.000(1)	2.267	Cg1: N3−C3−C9−C10−C11−C12
Cg2⋯Cg1 [1 − X, −Y, 1 − Z]	4.000(1)	1.808	Cg2: N4−C4−C8−C7−C6−C5
Cg3⋯Cg4 [2 − X, −Y, 1 − Z]	3.537(1)	0.785	Cg3: N13−C21−C27−C28−C29−C30
Cg4⋯Cg3 [2 − X, −Y, 1 − Z]	3.537(1)	1.033	Cg4: N14−C22−C26−C25−C24−C23

and Na$^+$ occupy only the inner part of this layer, and the anionic complexes $[W(CN)_6(bpy)]^{2-}$ are on its surface. Additionally, the network of hydrogen interactions present in the structure stabilizes the inorganic layer (Table 3).

Structure of 2 (NaRb). The compounds **1** and **2** show considerable structural similarity. As in the previously described structure, the asymmetric part of the unit cell of compound **2** contains an anionic complex molecule [W-(CN)$_6$(bpy)]$^{2-}$, rubidium and sodium atoms as counter ions, and five water molecules (Figure 5). In the asymmetric part of the unit cell of **2**, the Rb−W distance is 5.0234 (6) Å, while the Na−W distance is 5.4903 (13) Å. The immediate surroundings of the sodium cation are four water molecules and two cyanido "end-on" bridging nitrogen atoms (N15 and N14) (Figure 6).
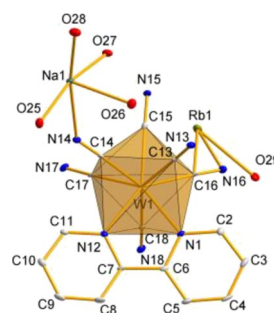
The Na$^+$ coordination environment adopts the geometry of a slightly distorted octahedron. The rubidium cation has a seven-coordinate environment with a highly distorted capped trigonal prism geometry. In the immediate vicinity of this cation, there are four water molecules (O26, O27, O28, and O29) and three cyanido ligands bridging in the "side-on" mode, C16N16, C15N15, and C17N17. Similar to structure **1**,

Table 3. Hydrogen Bonds for 1, 2, and 3

D−H⋯A	d(D−H) [Å]	d(H⋯A) [Å]	d(D⋯A) [Å]	∠(DHA) [deg]
1 Na/K				
O(5)−H(5AO)⋯N(13)#1	0.87	2.20	3.021(4)	157.0
O(5)−H(5BO)⋯N(14)#2	0.87	2.13	2.862(4)	141.6
O(6)−H(6BO)⋯N(17)#3	0.89	2.11	2.947(4)	156.7
O(6)−H(6AO)⋯N(15)	0.89	1.95	2.807(4)	162.3
C(8)−H(8)⋯O(5)#4	0.95	2.56	3.378(4)	144.8
C(10)−H(10)⋯N(13)#5	0.95	2.67	3.334(4)	127.0

#1 x,y,z+1; #2 x+1,y,z+1; #3 x−1,y,z; #4 −x+1,−y+1,−z+1; #5 −x,−y+1,−z

2 Na/Rb				
C(3)−H(3)⋯N(18)#4	0.95	2.57	3.299(4)	133.3
C(5)−H(5)⋯O(25)#5	0.95	2.57	3.403(4)	146.5
C(2)−H(2)⋯N(16)	0.95	2.65	3.272(5)	123.8
C(10)−H(10)⋯N(13)#6	0.95	2.62	3.362(5)	135.6
O(26)−H(26B)⋯N(18)#2	0.74(5)	2.21(5)	2.944(4)	174(5)
O(28)−H(28B)⋯O(29)#7	0.77(5)	2.06(5)	2.818(4)	167(4)
O(26)−H(26A)⋯N(13)	0.84(6)	2.29(6)	3.111(4)	165(5)
O(27)−H(27B)⋯N(17)#8	0.93(5)	2.05(5)	2.936(4)	159(4)
O(27)−H(27A)⋯N(15)	0.76(4)	2.51(4)	3.179(4)	149(4)
O(29)−H(29A)⋯N(13)#1	0.77(4)	2.11(4)	2.873(4)	168(4)
O(29)−H(29B)⋯N(14)#9	0.86(5)	2.13(5)	2.988(4)	174(4)
O(25)−H(25A)⋯N(16)#3	0.922(19)	1.98(2)	2.890(3)	169(4)
O(25)−H(25B)⋯N(18)#2	0.924(19)	2.20(3)	3.058(4)	154(5)

#1 x,y,z−1; #2 x,y,z+1; #3 x+1,y,z+1; #4 −x,−y+1,−z+1; #5 −x+1,−y+1,−z+2; #6 x+1,y,z; #7 x+1/2,−y+1/2,z+3/2; #8 x−1/2,−y+1/2,z+1/2; #9 x−1,y,z−1

3 Na/Cs				
C(6)−H(6)⋯N(16)#1	0.95	2.46	3.392(6)	166.2
C(9)−H(9)⋯N(5)#2	0.95	2.69	3.512(7)	144.8
C(11)−H(11)⋯N(15)#3	0.95	2.67	3.610(6)	172.1
C(27)−H(27)⋯N(11)#4	0.95	2.50	3.253(6)	135.7

#1 −x+2,−y,−z; #2 −x+1,−y,−z+1; #3 x−1,y,z+1; #4 −x+2,−y+1,−z

Figure 5. Asymmetric part of the unit cell of the compound **2** with the adopted numbering scheme. All H atoms are omitted for clarity. All nonhydrogen atoms are represented at 30% probability thermal ellipsoids. The coordination environment around the tungsten atom is in the shape of a slightly distorted dodecahedron.
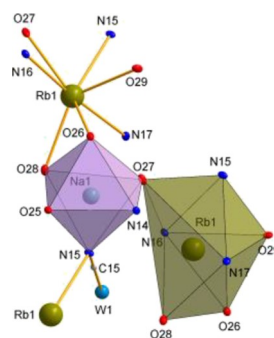
Figure 6. Relationship between cationic (Na⁺, Rb⁺) and anionic (W) metal centers. The figure shows the coordination environment of rubidium and sodium cations, and additionally the function of sodium ion as a " structure linker."
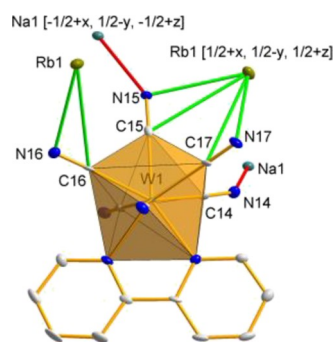
Figure 7. Anion bridge interactions $[W(CN)_6(bpy)]^{2-}$, in structure **2**. Green are "side-on" bridges to potassium cations, and red are "end-on" bridges to sodium cations.

this one can find cationic dimers Rb⁺-2H₂O-Na⁺, but this time the dimer is formed based on two bridging water molecules, O26 and O28. Identical to structure **1**, in structure **2**, only four out of six cyanido ligands of $[W(CN)_6(bpy)]^{2-}$ are involved in the formation of intermetallic bridges. C13N13 and C18N18 do not create any bridges, while C15N15 forms a bifurcated bridge, to Rb1 in the "side-on" mode and to Na1 in the "end-on" type. C14N14 also forms an "end-on" bridge to the sodium cation, while C16N16 and C17N17 "side-on" bridges to the rubidium cation (Figure 7).

As in **1**, the packing should also be distinguished in **2**, which adopts an organic−inorganic bilayer system with Miller indices (110). Sodium and rubidium cations form an inner layer in the

inorganic layer, while the organic layer is made up of bpy ligands of adjacent complex anions, which interact through π⋯π interactions (Table 2) to connect adjacent bilayers discussed later.

Structure of 3 (NaCs). In the asymmetric part of the unit cell of compound **3**, there are two anions $[W(CN)_6(bpy)]^{2-}$, four cations, including three Cs⁺ and one Na⁺, and seven water molecules, of which only one (O8) is water of crystallization, while the other six interact (coordinate) with cations (Figure 8).

Ion W(IV) adopts the square antiprismatic coordination environment described in the previous structures and does not show any significant differences from the already described systems (see Table S1). As presented in Figure 9, in **3** three
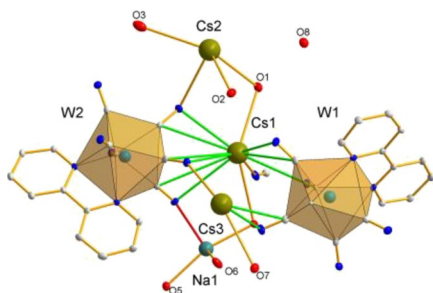
Figure 8. Asymmetric part of the unit cell of compound **3** with a simplified numbering scheme adopted for clarity. All H atoms are omitted for clarity. All nonhydrogen atoms (except Na, Cs, and W) are represented with 30% probability thermal ellipsoids.

different coordination modes of cesium are observed, with coordination numbers 11, 12, and 13 in one compound. The last coordination number is very rare as it was observed only once in the literature,[27] where Cs^+ is trapped in the cage of Ti cluster. The Cs1 atom is the central cation upon which the main network of bridging interactions is formed, linking the two $[W(CN)_6(bpy)]^{2-}$ anions into a dimeric arrangement in the asymmetric part of the unit cell (Figure 9a). Up to six cyanido bridges are formed to the Cs1 cation, 5 of which are of the "side-on" type (3 from W2 and 2 from W1) and one "end-on" type by the cyanido ligand C20N12 from the tungsten atom of W1 $[-1 + x, y, z]$.

The other cesium cations, Cs2 and Cs3, also exhibit an abundance of bridging interactions, as shown in Figure 9b,c. Three "side-on" and one "end-on" cyanido bridges are formed to the Cs2 cation, while four "side-on" and two "end-on" interactions are formed to the Cs3 cation. This wealth of bridging interactions is complemented by the presence of coordination water molecules, which gives an extremely rich picture of the interactions in which cesium cations are involved. This type of complex network of mutual interactions has not been observed before in any structure containing the anionic $[W(CN)_6(bpy)]^{2-}$ complex. The anionic complex based on the tungsten atom W1 is involved in the formation of numerous cyanido intermetallic bridges, in which only the bridge W1···C32N16···Cs3 $[2 - x, -y, -z]$ is of the "end-on" type, the rest is a "side-on" type, and additionally C20N12 is a

bridge bifurcated to Cs1 $[1 + x, y, z]$ and to Cs3. An interesting fact is that W1 does not interact directly with the Na1 cation and the cyanido ligand C31—N15, being perpendicular to the plane of the bpy ligand rings, as in the case of previously published compounds of this type[4,6,7] is not involved in any interactions of the bridging type. The W2-based complex anion is involved in similar interactions, but in this case two extremely rare trifurcation bridges, W2···C14N6 to: Cs1 ("side-on"), Na1 ("end-on") and Cs3 $[-1 + x, y, z]$ ("side-on") − Figure 10a and W2···C15N7 to: Cs1 ("side-on"), Cs3 ("end-on") and Cs2 $[2 - x, 1 - y, 1 - z]$ ("side-on") − Figure 10b.
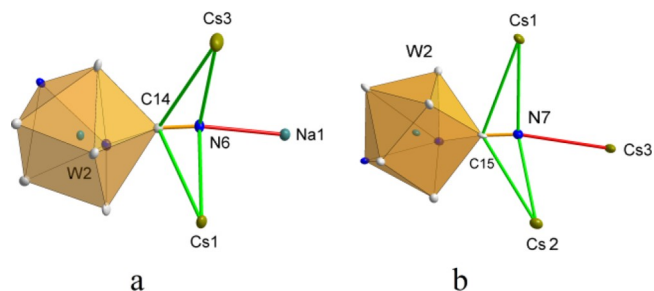
Figure 10. Rarely observed involvement of the cyanido ligand (C14N6 and C15N7) in the quadruple (trifurcated) interaction bridging the tungsten atom with four different cations: Cs1, Cs2, Cs3, and Na1.

This type of interaction between cyanides and alkali metal ions was observed earlier by Rauchfuss et al. in caged cyanometalates, where the cyanides bridging along the edge of the cage interact through weak electrostatic interactions also in "side-on" manner with the alkali metal cation trapped in the center of the cavity.[28−30] Similar interactions were also described in the work of Gokel et al., except that the side interactions concerned alkene/alkyne units and alkali metal cations.[31−34] Also, in our previous work on monocationic (K^+, Rb^+, and Cs^+) systems with $[W(CN)_6(bpy)]^{2-/-}$, "side-on" cyanide interactions have been described, which, in addition to the spatial arrangement and realization being obviously different from those cyanido interactions described herein, are additionally different in geometrical parameters. It should
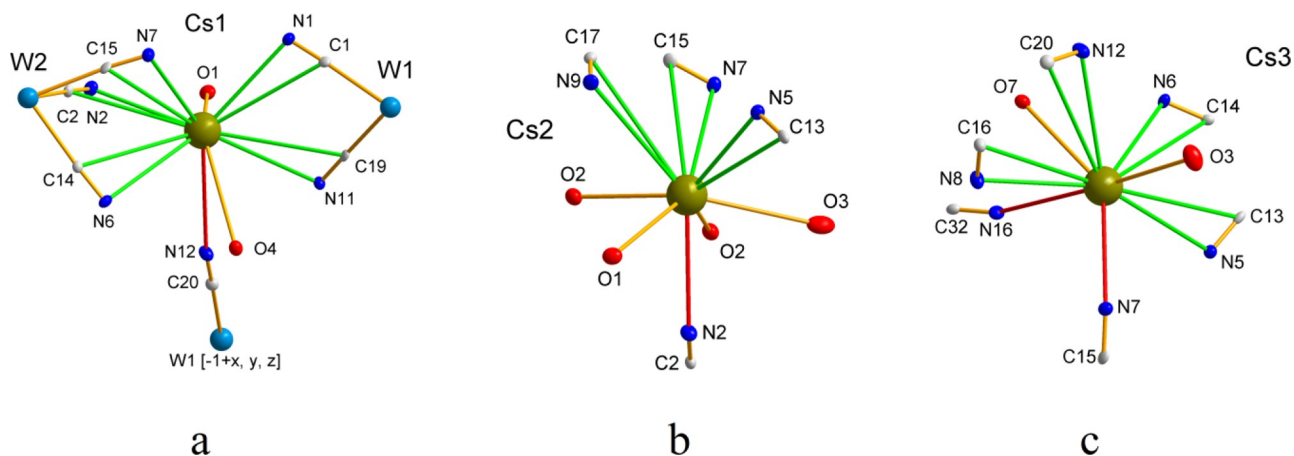

Figure 9. Coordination environment of the three cesium cations and the different bridging modes of the cyanide ligands observed in structure **3**. "Side-on" bridging interactions are shown in green and "end-on" bridging interactions in red. All atoms shown are represented on thermal ellipsoids with a probability of 30%.

Table 4. Thicknesses of the Inorganic A and Bpy (B) Layers [Å], in 1, 2, and 3 Compared to the Crystal Density and Ionic Radii Present in the Structures of Cations

layer	Na	K	Rb	Cs	Na/K (1)	Na/Rb (2)	Na/Cs (3)
inorganic layer A [Å][a]	7.248	7.278	6.791	6.964	7.138	7.366	6.950
bpy (organic) layer B [Å][b]	6.371	7.049	6.525	7.582	6.459	6.366	6.779
A + B [Å]	13.619	14.327	13.302	14.545	13.597	13.732	13.729
density [g/cm³]	1.875	1.976	2.221	2.533	1.898	2.025	2.267

[a]Measured as the distance from sublayer W_{up} of the layer A to sublayer W_{down} of the same layer. [b]Measured as the distance from sublayer W_{down} of the layer A to sublayer W_{up} of the next layer A.
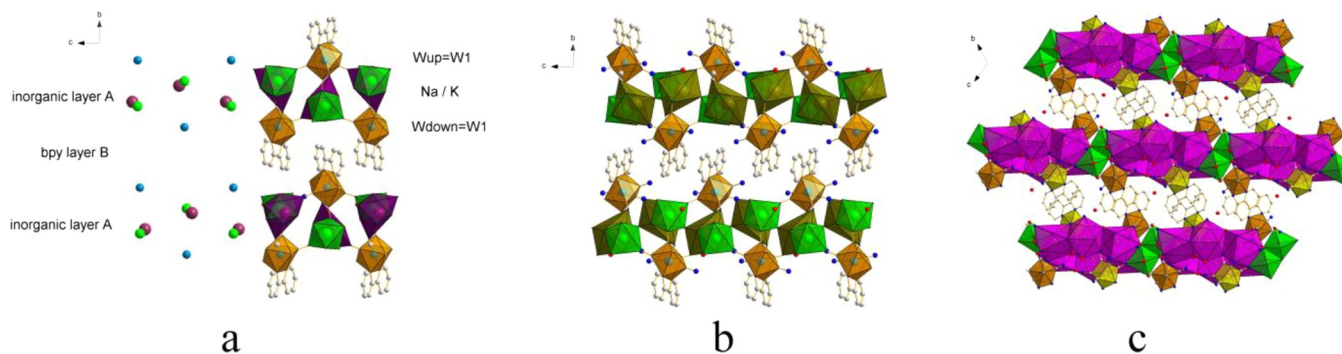
Figure 11. Scheme of the layered structure in structures **1**, **2**, and **3** (a−c, respectively). The sublayers W_{up} and W_{down} are marked in the figure. The orange color represents the coordination polyhedra of tungsten atoms W1 (in the case of structure **3**, the yellow color indicates the coordination polyhedron W2), the light green color represents coordination polyhedra of sodium cations, the pink color represents potassium cations, the dark green color represents rubidium cations, and the blue color represents cesium cations.

Table 5. Volumes of the Unit Cells Composed of Tungsten Atoms (V, in Å³) as Presented in Figure 12 in the Inorganic Layer[a]

	Na	K	Rb	Cs	Na/K (1)	Na/Rb (2)	Na/Cs (3)
x	8.647	8.458	8.810	8.812	8.242	8.418	9.308
y	8.677	8.500	9.233	9.039	9.201	10.326	9.719
z	9.951	9213	9.290	10.336	10.307	10.096	9.032
ω	56.43	111.20	60.20	51.27	62.85	125.23	61.31
ψ	96.85	68.86	116.42	128.59	103.39	102.47	85.81
τ	94.81	117.78	87.41	115.42	71.44	59.13	58.21
V	617.510	531.328	551.200	500.968	589.887	611.273	591.251

[a]For x, y, and z in angstroms and ω, ψ, and τ in degrees, where ω is the angle between y and z, ψ is the angle between x and z, and τ is the angle between x and y.

be noted that the cyanido interactions present in **1**, **2**, and **3**, of both "both side-on" and "end-on" types differ in geometry, from those found in previously published structures.[4,6,7] They are stronger as manifested by much shorter cation-N and cation-C distances.

For the first time among all known and described systems $[W(CN)_6(bpy)]^{2-}$, it was observed that a cyanido ligand, in this case C17N9, being perpendicular to the ring plane of the bpy ligand, was involved in the formation of the intermetallic bridge connection, in this case "side-on" to Cs2 $[2 - x, 1 - y, 1 - z]$. This type of connection was previously observed, but only in the case of compounds containing the $[W^V(CN)_6(bpy)]^-$ anion.[25]

Layered Structures of 1−3. Layer thickness data, inorganic (A) and bpy (B) for each compound, are shown in Table 4. The most striking observation is the lack of an intuitive effect of the size of the cation radius on the thickness of layer A and consequently B. One would expect that the introduction of a cation of increasing radius ($Cs^+ = 1.67$ [Å], $Rb^+ = 1.52$ [Å], $K^+ = 1.35$ [Å], $Na^+ = 1.02$ [Å])[35] into the structure, from K to Cs, would be associated with a stretching (increase) of the thickness of layer A. In the case of the

structures discussed, this effect is not seen, and to put it bluntly, when comparing the thickness of layer A of structures **1** and **3**, the effect is just the opposite! Correlating the thickness of layer A of individual compounds with their densities and ionic radii of the cations present in them, in the case of **3** the inorganic layer becomes more packed (Figure 11), indicating that as the ionic radius of the cation increases, the larger the cation the more easily its electron density becomes polarized; cyanido "side-on" bridging interactions begin to dominate in the structure. The introduction of smaller alkali metal cations into the structure further enhances this phenomenon compared to structures containing the same metal.[5−8] The observed phenomenon will also be affected by the presence of a large number of water molecules that penetrate the layer composed of stacked bpy molecules. The introduction of relatively strong (but not as strong as in the case of ion−ion interactions) hydrogen bonds reduces the thickness of the inorganic layer and causes an increase in the thickness of the bpy layer.

It can be seen that in the case of NaK and NaCs salts the A + B distance is smaller than that in both monocationic salts (Na and K or Na and Cs). It is especially well seen in **1** but

also in **3** assuming that we have three Cs^+ and only one Na^+ in complex formula. Such a decrease in the A + B distance indicates that in mixed alkali metal salts intermolecular forces are stronger and/or crystal packing is more compact. This is also supported by the A inorganic layer thickness which is smaller in mixed cation salts **1** and **3** than in monocationic salts. This may indicate why such salts are less soluble and start to precipitate from the mixed cation solution of complex. It must be stressed that anion−cation interactions interpreted in terms of the A + B (Table 4) distance are disturbed by the bpy−bpy interactions in the B layer. On the other hand, the A thickness does not directly correlate with the anion−cation forces, as the anion−anion distance spread not only vertically (A thickness) but also horizontally along the inorganic layer. In Table 5, we present the W−W distances and angles as well as volume of the polyhedron composed of eight adjacent tungsten atoms (4 on the bottom and 4 on the top of the inorganic layer) as presented in Figure 12. This volume reflects the "compression" of the inorganic layer.
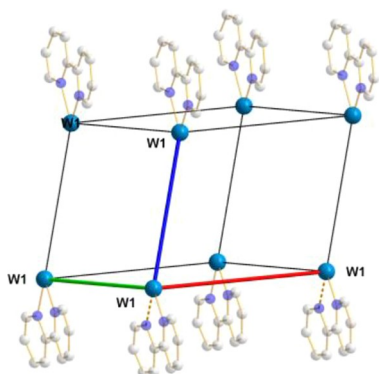
Figure 12. Polyhedron formed on the tungsten atom in **1**. The water molecules, hydrogen atoms, and potassium cations are omitted for clarity. The colors are *x*, *y*, and *z*. It does not matter which color or designation is assigned to an edge, but note that when calculating the volume of such a diagonal solid, the angular relationships between the edges must be maintained (Table 5).

In Table 5, it can be seen that the volume *V* of the inorganic layer for monocationic salts unexpectedly decreases on going from Na to Cs salt with an unusual change for K salt. This is an opposite direction than that observed for cation radii. The lowest volume has the cesium salt with volume lower by 19% than that of sodium one. Such a behavior could be interpreted as the decrease of the W-cation distance, due to "side-on" bonding of cations to CN ligands starting from potassium salts, but this is not a sufficient explanation as the shortest Na−W distance is 4.925 Å, K−W 3.940 Å, Rb−W 4.791 Å, and Cs−W 5.125 Å respectively which does not reflect the *V* value change given in Table 5. Also the average cation-W distances (calculated as average from all W-cation distances from the first anion−cation coordination sphere) equal to 5.795, 5.433, 5.184, and 5.640 Å for Na, K, Rb, and Cs salts do not follow the *V* volume change, at least for the Cs cation. As on going from K to Cs cation, one observes an increase in its polarity, and thus the heavier cation can, as it were, be deeper pressed into the anion's surroundings, thereby better and more uniformly compensating for its charge, resulting in a decrease in the electrostatic repulsion of the anion−anion and thus a decrease in the volume value of the unit cell. It is worth to indicate also that the cation radii do not increase significantly

on going from K^+ to Cs^+ at the coordination number present in those salts (from 1.55, 1.63 to 1.81 Å for K^+, Rb^+, and Cs^+ respectively). For mixed cation salts **1−3**, the V volume is lower for all mixed cation salts **1−3** compared to $Na_2[W-(CN)_6(bpy)]$ salt.[7] This is why the sodium salts tend to convert into mixed cation salts.

CONCLUSIONS

The formation of mixed cation salts is often observed in inorganic compounds. There is no information what is the reason of such salt formation. For the first time, we have a unique opportunity to isolate good-quality crystals of monocationic and mixed cationic salts and thus to compare the monocrystalline structures of these two types of salts. The data presented here indicate that the presence of not only sodium but also large easily polarizable cations (K, Rb, and Cs) provides the opportunity for better spatial compensation of the anion charge, resulting in more compactly packed crystals. The presence of cations with different properties allows for an increased number of intermolecular interactions in the mixed cationic salts, resulting in denser spatial ordering of the molecules. This affects the lower solubility compared to single-cation systems, so they can be obtained from sodium, potassium, rubidium, and cesium salts. Thus, the more stable structure of mixed cationic salts is responsible for their crystallization, probably also in other known systems.

ASSOCIATED CONTENT

ⓈⒾ Supporting Information

The Supporting Information is available free of charge at https://pubs.acs.org/doi/10.1021/acs.cgd.2c00540.

Selected crystal structure data (Table S1) as well as IR spectra (Figures S1, S2, and S3) (PDF)

Accession Codes

CCDC 1908247, 2113721, and 2113722 contain the supplementary crystallographic data for this paper. These data can be obtained free of charge via www.ccdc.cam.ac.uk/data_request/cif, or by emailing data_request@ccdc.cam.ac.uk, or by contacting The Cambridge Crystallographic Data Centre, 12 Union Road, Cambridge CB2 1EZ, U.K.; fax: +44 1223 336033.

AUTHOR INFORMATION

Corresponding Author

Maciej Hodorowicz − *Faculty of Chemistry, Jagiellonian University, 30-387 Kraków, Poland;* ⓞ orcid.org/0000-0003-4210-3625; Email: hodorowm@chemia.uj.edu.pl

Authors

Janusz Szklarzewicz − *Faculty of Chemistry, Jagiellonian University, 30-387 Kraków, Poland;* ⓞ orcid.org/0000-0001-9747-9238

Anna Jurowska − *Faculty of Chemistry, Jagiellonian University, 30-387 Kraków, Poland;* ⓞ orcid.org/0000-0001-6562-0954

Complete contact information is available at:
https://pubs.acs.org/10.1021/acs.cgd.2c00540

Author Contributions

The manuscript was written through contributions of all authors. All authors have given approval to the final version of the manuscript.

Notes

The authors declare no competing financial interest.

■ REFERENCES

(1) Beevers, C. A.; Hughes, W. The crystal structure of Rochelle salt (sodium potassium tartrate tetrahydrate $NaKC_4H_4O_6 \cdot 4H_2O$). *Proc. R. Soc. London, Ser. A* **1941**, *177*, 251−259.

(2) Samotus, A.; Dudek, M.; Kanas, A. Dioxotetracyano-complexes of molybdenum(IV) and tungsten(IV) and their vibrational spectra. *J. Inorg. Nucl. Chem.* **1975**, *37*, 943−948.

(3) Dudek, M.; Samotus, A. Oxopentacyano-complexes of molybdenum(IV) and tungsten(IV) in photolysis of octacyanometalates(IV). *Transition Met. Chem.* **1985**, *10*, 271−274.

(4) Szklarzewicz, J.; Fawcett, J.; Russell, D. R. Synthesis and X-ray crystal structures of $Cs_2[W(bpy)(CN)_6] \cdot 2H_2O$ and $(AsPh_4)_2[W-(bpy)(CN)_6] \cdot 3.5H_2O$. *Transition Met. Chem.* **2004**, *29*, 56−60.

(5) Hodorowicz, M.; Szklarzewicz, J.; Jurowska, A. The versatility of lithium cation coordination modes in salts with $[W(CN)_6(bpy)]^{2-}$ anions. *CrystEngComm* **2020**, *22*, 3991−3998.

(6) Hodorowicz, M.; Jurowska, A.; Szklarzewicz, J. X-ray crystal structures of K^+ and Rb^+ salts of $[W(CN)_6(bpy)]^{2-}$ ion. The unusual cation−anion interactions and structure changes going from Li^+ to Cs^+ salts. *CrystEngComm* **2021**, *23*, 1207−1217.

(7) Hodorowicz, M.; Jurowska, A.; Szklarzewicz, J. Unusual structural changes going from Li^+ to Cs^+ in $[W(CN)_6(bpy)]^{2-}$ ion salts: the Na^+ case. *CrystEngComm* **2021**, *23*, 4301−4311.

(8) Hodorowicz, M.; Szklarzewicz, J.; Jurowska, A.; Mikuriya, M.; Mitsuhashi, R.; Yoshioka, D. Cation versus weak intermolecular interactions in the structures of Et_4N^+, Pr_4N^+, and Bu_4N^+ cation salts with the $[W(CN)_6(bpy)]^{2-}$ anion. *J. Struct. Chem.* **2021**, *62*, 905.

(9) Ma, S. L.; Ren, S.; Ma, Y.; Liao, D. Z.; Yan, S. P. Three types of heterometallic structural motifs based on $[Mo(CN)_8]^{3-/4-}$ anion and Mn^{II} cation as building blocks. *Struct. Chem.* **2009**, *20*, 145−154.

(10) Kumar, K.; Stefanczyk, O.; Nakabayashi, K.; Imoto, K.; Ohkoshi, S. I. Studies of Er(III)−W(V) compounds showing nonlinear optical activity and single-molecule magnetic properties. *CrystEngComm* **2019**, *21*, 5882−5889.

(11) Zhou, H.; Diao, G. W.; Yang, X. Z.; Yuan, A. H.; Zhang, M.; Sun, J. Further Insights into the Role of Temperature in the Synthesis of the Lanthanide(III)-Pyrazine-Octacyanotungstate(V) System: an Example of Discrete Materials. *Z. Anorg. Allg. Chem.* **2013**, *639*, 2276−2281.

(12) Imoto, K.; Nakagawa, K.; Miyahara, H.; Ohkoshi, S. I. Super-Ionic Conductive Magnet Based on a Cyano-Bridged Mn−Nb Bimetal Assembly. *Cryst. Growth Des.* **2013**, *2013*, 4673−4677.

(13) Mallah, T.; Thiébaut, S.; Verdaguer, M.; Veillet, P. High-T_c Molecular-Based Magnets: Ferrimagnetic Mixed-Valence Chromium-(III)-Chromium(II) Cyanides with T_c at 240 and 190 Kelvin. *Science* **1993**, *262*, 1554−1557.

(14) Sato, O.; Iyoda, T.; Fujishima, A.; Hashimoto, K. Photoinduced magnetization of a cobalt-iron cyanide. *Science* **1996**, *272*, 704−705.

(15) Ohkoshi, S.; Tokoro, H.; Matsuda, T.; Takahashi, H.; Irie, H.; Hashimoto, K. Coexistence of ferroelectricity and ferromagnetism in a rubidium manganese hexacyanoferrate. *Angew. Chem., Int. Ed.* **2007**, *119*, 3302−3305.

(16) Jafri, S. F.; Arrio, M. A.; Bordage, A.; Moulin, R.; Juhin, A.; Moulin, C. C.; Otero, E.; Ohresser, P.; Bleuzen, A.; Sainctavit, P. Weak Ferromagnetic Interaction at the Surface of the Ferrimagnetic $Rb_2Co_4[Fe(CN)_6]_{3.3} \cdot 11H_2O$ Photoexcited State. *Inorg. Chem.* **2018**, *57*, 7610−7619.

(17) Felts, A. C.; Slimani, A.; Cain, J. M.; Andrus, M. J.; Ahir, A. R.; Abboud, K. A.; Meisel, M. W.; Boukheddaden, K.; Talham, D. R. Control of the speed of a light-induced spin transition through mesoscale core−shell architecture. *J. Am. Chem. Soc.* **2018**, *140*, 5814−5824.

(18) Lapidus, S. H.; Stephens, P. W.; Kareis, C. M.; VanNatta, P. E.; Miller, J. S. Anomalous Stoichiometry and Antiferromagnetic Ordering for the Extended Hydroxymanganese(II) Cubes/Hexacya-nometalate-Based 3D-Structured $[Mn^{II}_4(OH)_4][Mn^{II}(CN)_6](OH_2)_6 \cdot H_2O$. *Chem. − Eur. J.* **2019**, *25*, 1752−1757.

(19) Szklarzewicz, J.; Samotus, A. A novel cyano complex of tungsten (IV) with 2, 2′-bipyridyl. *Transition Met. Chem.* **1988**, *13*, 69−71.

(20) Szklarzewicz, J.; Samotus, A. Photochemical reactions of molybdenum and tungsten octacyanometallates (IV) in acidic aqueous media containing 2,2′-bipyridyl or 1,10-phenanthroline. *Transition Met. Chem.* **1995**, *20*, 174−178.

(21) Rigaku Oxford Diffraction. *CrysAlis PRO*; Rigaku OxfordDif-fraction: Yarnton, England, 2015.

(22) Sheldrick, G. M. Crystal structure refinement with SHELXL. *Acta Crystallogr., Sect. C: Struct. Chem.* **2015**, *C71*, 3−8.

(23) Sheldrick, G.M. *SHELX2017, Programs for crystal structure determination*; Universität Göttingen: Göttingen, Germany, 2017.

(24) Putz, H.; Brandenburg, K. *Diamond-Crystal and Molecular Structure Visualization Crystal Impact*; GbR: Bonn, Germany.

(25) Hodorowicz, M.; Jurowska, A.; Szklarzewicz, J. Structures of alkali metal salts with $[W(CN)_6(bpy)]^-$ ion. Comparative studies to W(IV) analogues. *Polyhedron* **2021**, *207*, No. 115369.

(26) Kepert, D. *Inorganic Stereochemistry, Inorganic Chemistry Concepts 6*; Springer, 1982; pp 117−129.

(27) Zhang, G.; Li, W.; Liu, C.; Jia, J.; Tung, C. H.; Wang, Y. Titanium-oxide host clusters with exchangeable guests. *J. Am. Chem. Soc.* **2018**, *140*, 66−69.

(28) Contakes, S. M.; Rauchfuss, T. B. Alkali metal-templated assembly of the tetrahedral cyanometallate cages $[M \subset Mo_4(\mu-CN)_6(CO)_{12}]^{5-}$ (M = Li, Na). *Chem. Commun.* **2001**, 553−554.

(29) Contakes, S. M.; Rauchfuss, T. B. $\{K \subset [Mo_6(\mu-CN)_9(CO)_{18}]\}^{8-}$: A Trigonal-Prismatic Cyanometalate Cage. *Angew. Chem., Int. Ed.* **2000**, *39*, 1984−1986.

(30) Kuhlman, M. L.; Rauchfuss, T. B. Structural Chemistry of "Defect" Cyanometalate Boxes: $\{Cs \subset [CpCo(CN)_3]_4[Cp^*Ru]_3\}$ and $\{M \subset [Cp^*Rh(CN)_3]_4[Cp^*Ru]_3\}$ (M = NH_4, Cs). *J. Am. Chem. Soc.* **2003**, *125*, 10084−10092.

(31) Hu, J. X.; Barbour, L. J.; Gokel, G. W. Cation-π Interactions Between Alkali Metal Cations and Neutral Double Bonds. *Collect. Czech. Chem. Commun.* **2004**, *69*, 1050−1062.

(32) Hu, J.; Gokel, G. W. Solution complexation between potassium iodide and lariat ethers having pi-donor sidearms. *Chem. Commun.* **2003**, 2536−2537.

(33) Gokel, G. W. The aromatic sidechains of amino acids as neutral donor groups for alkali metal cations. *Chem. Commun.* **2003**, 2847−2852.

(34) Hu, J.; Barbour, L. J.; Gokel, G. W. Solid-state evidence for π-complexation of sodium and potassium cations by carbon−carbon triple bonds. *J. Am. Chem. Soc.* **2001**, *123*, 9486−9487.

(35) Shannon, R. D. Revised effective ionic radii and systematic studies of interatomic distances in halides and chalcogenides. *Acta Crystallogr., Sect. A: Cryst. Phys., Diffr., Theor. Gen. Crystallogr.* **1976**, *32*, 751−767.